ARTICLE

Ultrafast Excited State Dynamics of *trans*-4-Aminoazobenzene Studied by Femtosecond Transient Absorption Spectroscopy[†]

Ya-ping Wang, Song Zhang[*], Si-mei Sun, Kai Liu, Bing Zhang[*]

State Key Laboratory of Magnetic Resonance and Atomic and Molecular Physics, Wuhan Institute of Physics and Mathematics, Chinese Academy of Sciences, Wuhan 430071, China

The ultrafast excited state dynamics of *trans*-4-aminoazobenzene (*trans*-4-AAB) in ethanol was investigated by femtosecond transient absorption spectroscopy. After being excited to the S_2 state by 400 nm, *trans*-4-AAB decays from the S_2 state to the hot S_1 state by internal conversion with time constant of $\sim$70 fs. The photoisomerization through inversion mechanism on the S_1 potential energy surface and the internal conversion from the S_1 state to the hot S_0 state are observed, respectively. The average timescale of these two decay pathways is $\sim$0.7 ps. And the vibrational cooling of the hot S_0 state of *cis*- and *trans*-4-AAB occur with time constants of $\sim$4 and $\sim$13 ps, respectively. Furthermore, the ultrafast intersystem crossing process are also observed. The timescale of intersystem crossing from the S_2 state to the T_4 state is about 480 ps while from the S_1 state to the T_2 state is $\sim$180 ps.

Key words: Photoisomerization, *trans*-4-AAB, Femtosecond transient absorption spectroscopy, Intersystem crossing

I. INTRODUCTION

The *trans-cis* photoisomerization reactions of azobenzene and its derivatives have been investigated in several decades. The molecular dipole, absorption spectrum, dielectric constant, refractive index, and structure would be changed when photoisomerization occurs. It provides wide applications in optical information processing, light-driven switch, and nonlinear optics [1−6]. Therefore, further understanding of the reaction dynamics of the *trans-cis* photoisomerization behavior is necessary to realize the application of azobenzene and its derivatives as optical materials.

Quantum chemistry calculation and various spectroscopies, such as steady-state spectroscopy, transient absorption spectroscopy, and time-resolved Raman spectroscopy, *etc.* have been used to investigate the *trans-cis* photoisomerization of azobenzene and its derivatives [7−24]. In the steady-state spectrum, *trans*-azobenzene is characterized by two absorption bands: a weak n-π^* absorption at 440 nm known as the S_1 state and a strong π-π^* absorption at 320 nm known as the S_2 state [1]. Excitation to the S_1 state is believed to result in the isomerization by inversion mechanism which involves in-plane bending of a CNN bond angle [8, 12]. However, UV excitation to the higher-energy S_2 state, the

isomerization mechanism of *trans*-azobenzene is controversial. Some scientists think the rotational isomerization, which is caused by a rotating around the N=N double bond, is dominated for excitation to the S_2 state [13, 14]. It is similar to the mechanism isomerization dynamics observed for stilbenes [15]. But others think the isomerization takes place by an inversion mechanism on the S_1 potential energy surface after the internal conversion from the S_2 state to the planar S_1 state [16]. In 1998, Moore and his co-workers studied the isomerization of *trans*-azobenzene by femtosecond time-resolved UV-visible absorption spectroscopy [13]. They concluded that when *trans*-azobenzene is excited to the S_2 (π-π^*) state, it decayed to the S_1 state via a fast internal conversion by 0.9 ps and the photoisomerization occurred on the S_1 potential energy surface within 15 ps. But Ikeda and his co-workers have researched a liquid crystalline *trans*-azobenzene (4-butyl-4-methoxyazobenzene, abbreviated as BMAB) in solution by femtosecond transient absorption and picosecond single-photon timing fluorescence spectroscopies, but concluded the different decay times of the excited states [21]. Their results indicate that after excitation to the S_2 state, a fast internal conversion from the S_2 state to the S_1 state occurs within 200 fs. The photoisomerization occurs on the S_1 potential energy surface and the time scale is $\sim$1 ps. In 1980, Schulte-Frohllnde and his co-workers studied a series of *trans*-azobenzenes substituted by nitro and dialkylamino groups in the 4 and 4′ positions or additional polar groups by a laser flash photolysis [18]. They observed directly the existence of the triplet state of azobenzene for the first

---

time. Formation and decay of the observed triplet states depend on the nature of the substituent and the solvent. Then Angelo *et al.* studied the quantum yield of the triplet states of 4-diethylaminoazobenzene and 4-diethylamino-4′-met-hoxyazobenzene by irradiation of the pyrex-filtered light [19]. It is concluded that the π-π* singlet states undergo efficient intersystem crossing to the high-lying triplets and the lowest excited singlet state S_1 undergoes minimal intersystem crossing into the T_1 state. For other azobenzene's derivatives, intersystem crossing into the triplet states isn't observed up to now. As demonstrated here, an interesting and somewhat puzzling aspect of excited-state isomerization mechanism, time scale of excited-state decay and the character of triplet states arise.

In this work, we have investigated the ultrafast excited state dynamics of a substituted *trans*-azobenzene, *trans*-4-aminoazobenzene (*trans*-4-AAB) in ethanol through excitation to the S_2 state by femtosecond transient absorption spectroscopy. After excitation by 400 nm, the decay dynamics of the S_2 and S_1 states and the photoisomerization on the S_1 potential energy surface were observed respectively. Furthermore, the ultrafast intersystem crossing process was also observed.

II. EXPERIMENTS AND CALCULATION

trans-4-AAB (98% purity) was purchased from Sigma and used without further purification. Ethanol purchasing from Aladdin (99% purity) was used as solvent. The concentration of *trans*-4-AAB in ethanol was 1 mmol/L at room temperature and a fresh sample was prepared for each experiment.

The ultrafast transient absorption setup is based on a regenerative amplified femtosecond laser system. Details of this system have been described before [25]. Briefly, the seed beam was generated by a commercial Ti:sapphire oscillator pumped by a CW second harmonic of an Nd:YVO$_4$ laser. A 1 kHz regenerative amplifier was used to generate 35 fs pulses at 800 nm with an energy of 1 mJ/pulse as fundamental pulse. Excitation light at 400 nm is the second harmonic generation of the fundamental pulse obtained by a 1 mm thick BBO crystal. The pump pulse energy at the sample is less than 5 μJ with a diameter of about 0.5 mm for measurements. A portion of the fundamental pulse was focused into a 1 mm thick Sapphire to generate a white continuum (440−690 nm). In order to improve the measuring sensitivity, the white light was split into the probe and the reference beam by a metallic-coated beamsplitter. And the polarization angle between the pump and the probe beam is set at the magic angle (54.7°). Approximately 20 mL of the solution was held in a flow cell with 0.2 mm quartz windows and 1 mm optical path length. The cell was spun at several hundred round per minute about its axis to avoid reexcitation of the pumped volume by successive laser pulses. The

pump and probe pulses spatially overlapped in the sample at an intersection angle of ∼5°, and the reference beam was transmitted through the sample at a different spot. The probe pulse was temporally delayed with respect to the pump pulse through a computer controlled translation stage (HWHR, MC400) which was put on the path of probe light, with a resolution of ∼1.04 fs. Three optical shutters are used to block the fundamental, pump and probe pulse regularly. A CCD camera (PI-MAX, 1024×256 pixel array) equipped with a spectrometer (Princeton, SpectraPro 2500i) was used to collect the probe and reference pulses. The readout of the CCD-array, the delay stage, and the various shutters *etc.* were controlled by a LabView program on a PC. Each of the recorded spectra is accumulated on the CCD for typically 1600 laser shorts. The instrumental response of the system was determined to be ∼200 fs by cross-correlation measurements between pump and probe pulse. The cross-correlation function was also used to determine the precise zero time-delay at each probe wavelength.

All quantum chemical calculations were carried out with the Gaussian 09 software package [26]. The geometry of the S_0 state was optimized at the B3LYP functional level with the 6-311++G(d,p) basis set. Vertical transition energies and oscillator strengths of the excited states of *trans*- and *cis*-4-AAB were determined by the time-dependent density functional theory (TD-DFT) with the 6-311++G(d,p) basis set.

III. RESULTS AND DISCUSSION

In the steady-state absorption spectrum of *trans*-4-AAB in ethanol, there are two characteristic absorption bands: a strong π-π* band with the center wavelength at 390 nm and a weak n-π* band with the center wavelength at 440 nm [24]. According to the computed result, the oscillator strengths of $S_1 \leftarrow S_0$ and $S_2 \leftarrow S_0$ transition are 0.0 and 0.8095, respectively. It indicates that one-photon excitation is optically forbidden to the S_1 state, but optically allowed to the S_2 state. The vertical transition energies of the S_1 and S_2 states are 2.56 eV (∼480 nm) and 3.65 eV (∼340 nm), respectively, which are similar to the experimental results. And the vertical transition energies of the first four excited triplet states are 1.81, 2.20, 3.45, and 3.60 eV, respectively. According to the steady-state absorption spectrum and calculations, *trans*-4-AAB can be excited into the S_2 state by 400 nm.

In order to obtain complete information as more as possible on the dynamics of *trans*-4-AAB, the change of the optical density was measured until the delay time between pump and probe laser is up to 90 ps. Two-dimensional transient absorption spectrum of *trans*-4-AAB in the 440−690 nm following excitation by 400 nm is shown in Fig.1. The spectrum presented here can be divided into four regions and each of them contains different dynamical processes. The blue region from
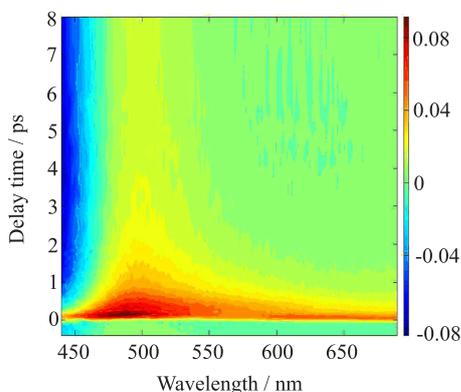
FIG. 1 Two-dimensional transient absorption spectrum of *trans*-4-AAB in ethanol with delay time up to 8 ps following excitation at 400 nm.

440 nm to 470 nm is negative signal and elucidated by the overlapping of the ground-state bleach and the absorption of the $S_n \leftarrow S_1$ state. In the 470−530 nm, after the first 2 ps the signal maintains ∼0.02 until the decay time was up to 90 ps. It is reasonable to assume that the photoisomerization to *cis*-4-AAB occurs and *cis*-isomer thermally converts back to *trans*-4-AAB on a much longer timescale. Furthermore, the signal intensity evolves fast in the first 2 ps due to the decay of the S_1 state. In the range of 530−600 nm, the red signal is illustrated by the absorption of the $S_n \leftarrow S_1$ state only and in the 600−690 nm, the red signal is illustrated by the absorption of the S_1 and S_2 states. From Fig.1, we can notice that the signal in 600−690 nm is stronger than that in 530−600 nm in the first ∼0.2 ps and afterwards attenuates to the same amplitude. It indicates that the decay of the S_2 state may complete within ∼0.2 ps.

The time evolutions of the optical density of *trans*-4-AAB in ethanol at all probe wavelengths were fitted by the exponential function convoluted with the response function of the instrument. All the time constants determined by fitting are presented in Table I. The evolution of the optical density observed in 600−690 nm was well fitted by triple-exponential function and the three timescales are about 70 fs (τ_1), 0.6 ps (τ_2), and 480 ps (τ_3), respectively. The decay times τ_1 and τ_2 are assigned to the decay of the S_2 and S_1 states, respectively. But the longer time τ_3 is a new component and has not been discussed in ultrafast timescale before. In the range of 530−600 nm, the evolution in the optical density was well fitted by double-exponential function. The time constants are ∼0.7 ps (τ_2) and ∼180 ps (τ_4), respectively. But the decay component of 70 fs was not observed here. The 0.7 ps-component is assigned to the decay of the S_1 state but the longer time constant τ_4 is a new component and will be discussed later. In 470−530 nm, the weak signal with intensity of ∼0.02 exists all the time and is assigned to the absorption of *cis*-4-AAB. To eliminate the effect of this permanent

photoproduct in the optical density at long delay times, a time constant of 10 ns is included. Triple-exponential function was used to fit the time evolution of the optical density in this range and the timescales are ∼0.7 ps (τ_2) and ∼4.0 ps (τ_5). Because of the overlapping between ground-state bleach and excited-state absorption, the time evolution of the optical density between 440 and 470 nm was well fitted by double-exponential function. The time constants of these two decay components are ∼0.7 ps (τ_2) and ∼13 ps (τ_6), respectively. Figure 2 shows the time evolution of the optical density at selected probe wavelengths of 660, 580, 520, and 445 nm, respectively.

We first assigned the 70 fs-component (τ_1) observed in 600−690 nm as the internal conversion from the S_2 state to the hot S_1 state. Like 660 nm in this range, the inset of the Fig.2(a) shows that τ_1 decays with the appearance of τ_2. That exactly proves above conclusion. And similar results can also be seen in the photoisomerization of other azobenzene derivatives [11, 13, 19, 23, 24].

The time constant of ∼0.7 ps (τ_2) which is seen in all probe wavelengths is assigned to the average timescale of two decay pathways: a photoisomerization to *cis*-4-AAB by inversion mechanism and an internal conversion to the high vibrational state of the S_0 state. The signal of ∼0.02 at long delay time and the partial recovery of the bleach signal in the Fig.2(d) indicate that the photoisomerization to *cis*-4-AAB occurs. In order to make the isomerization mechanism on the S_1 potential energy surface clear, Moore and co-workers studied an azobenzene derivative in which azobenzene was capped by an azacrownether [11]. The "capped" azobenzene derivative cannot isomerize by torsional mechanism because large-scale motion of the phenyl groups is restricted by their linkage to azacrown ether. In this case, the photoisomerization process was still observed and azobenzene derivative was isomerized by inversion mechanism on the S_1 potential energy surface. From the above, we considered that the photoisomerization of *trans*-4-AAB happened on the S_1 potential energy surface by an inversion mechanism during the ∼0.7 ps.

The decay time τ_5 observed in 470−530 nm is ∼4 ps. The excited-state energies of *cis*-4-AAB in ethanol were predicted by the TD-DFT calculation at the B3LYP method. The first absorption peak of *cis*-4-AAB is in 470−530 nm. This range is corresponding to the probe wavelength at which τ_5 was observed. According to this, we assigned the decay time τ_5 to the vibration relaxation of the ground-state *cis*-4-AAB.

In 1983, Pietra and his co-workers studied the quantum yield of the triplet states of 4-diethylaminoazobenzene and 4-diethylamino-4′-methoxyazobenzene by irradiation of the pyrex-filtered light [19]. It was concluded that the π-π^* singlet states and the lowest excited singlet state undergo efficient intersystem crossing to the triplets. But the time-resolved results weren't shown. Here we assigned the compo-

TABLE I Kinetic parameters determined from analysis of the experimental data of *trans*-4-AAB in ethanol with delay time up to 90 ps. Preexponential factors a_i of the corresponding decay components are normalized as $\sum |a_i|=1$.

Wavelength/nm	a_1	τ_1/fs	a_2	τ_2/ps	a_3	τ_3/ps	a_4	τ_4/ps	a_5	τ_5/ps	a_6	τ_6/ps
680	0.75	66	0.19	0.8	0.06	442						
660	0.61	77	0.33	0.6	0.06	498						
620	0.37	61	0.57	0.6	0.06	442						
580			0.90	0.7			0.10	178				
560			0.92	0.7			0.08	174				
540			0.91	0.7			0.09	173				
530			0.78	0.7					0.17	4.2		
500			0.81	0.7					0.06	4.1		
490			0.83	0.7					0.02	3.7		
445			0.81	0.6							0.19	13
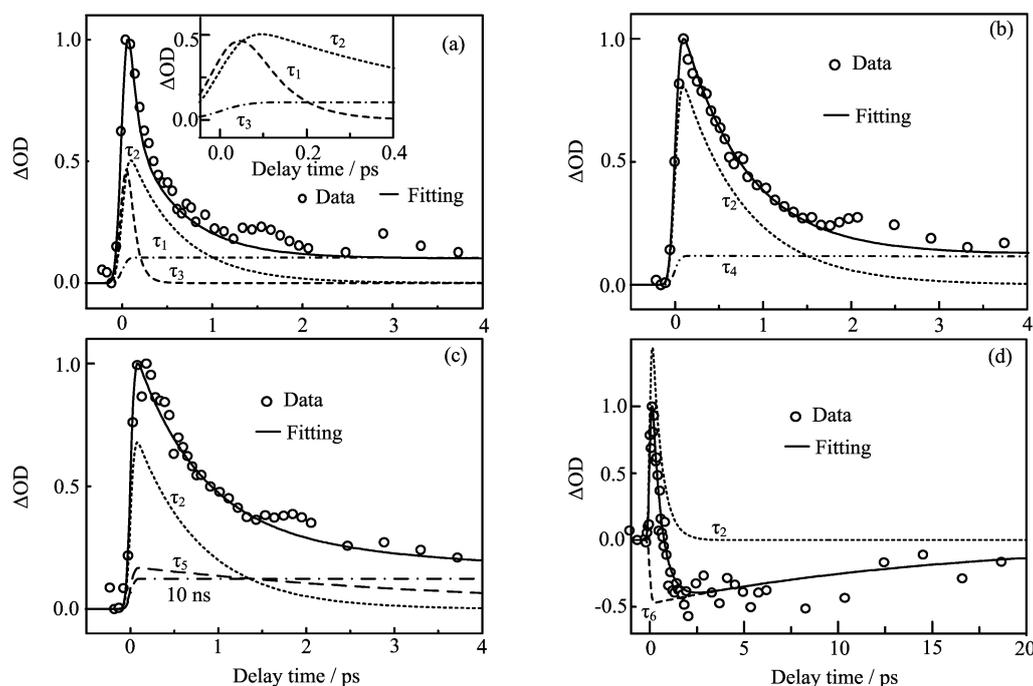
FIG. 2 Time evolution of the optical density of *trans*-4-AAB in ethanol at the selected probe wavelengths: (a) 660 nm, (b) 580 nm, (c) 530 nm, (d) 445 nm. The inset of (a) is the time components with short delay time.

nent of ~480 ps (τ_3) observed at probe wavelengths longer than 600 nm as an intersystem crossing to the triplet state. According to the calculation, the vertical transition energies of the T_4 and S_2 states are 3.60 and 3.65 eV, respectively. Considering to the energy gap rules, an intersystem crossing between the S_2 and T_4 states may be quite efficient. The time constant of ~180 ps (τ_4) observed in the range of 540−600 nm is assigned to the timescale of an intersystem crossing from the S_1 state to the triplet state. By means of calculation, the vertical transition energies of the T_2 and S_1 states are 2.20 and 2.56 eV, respectively. Considering to the energy gap rules, an intersystem crossing between the S_1 and T_2 states may be quite efficient.

In the range of the 440−470 nm, because of the over-

lapping of the ground-sate bleach and the absorption of the S_1 state, the time evolution of the optical density shows two decay components of ~0.7 ps (τ_2) and ~13 ps (τ_6). The decay time τ_6 is assigned to the vibration relaxation of the ground-state *trans*-4-AAB. According to the time-resolved infrared spectroscopy, the timescale of the vibrational cooling in the ground state of *trans*-azobenzene was ~20 ps [17], which was completely consistent with our result.

IV. CONCLUSION

The ultrafast excited-state dynamics of a substituted *trans*-azobenzene, *trans*-4-aminoazobenzene (*trans*-4-AAB) in ethanol was studied by femtosecond transient
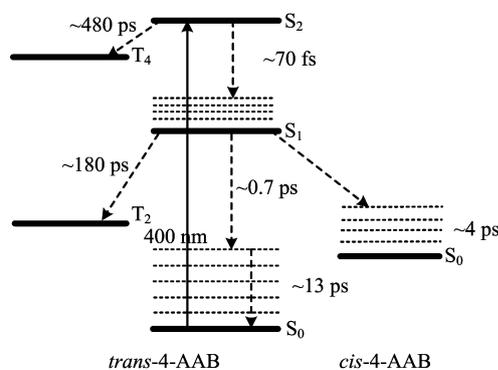
FIG. 3 The general photoinduced mechanisms for the S_2-excited *trans*-4-AAB.

absorption spectroscopy. A general photoinduced mechanism for the S_2-excited *trans*-4-AAB is deduced according to the experimental results and quantum chemical calculations, shown in Fig.3. After excitation to the S_2 state by 400 nm, two decay processes of *trans*-4-AAB were observed: one is a fast internal conversion to the hot S_1 state with timescale of $\sim$70 fs, and the other is an intersystem crossing to the T_4 state with timescale of $\sim$480 ps. The S_1 state decays with a dominant component of $\sim$0.7 ps and a weaker component of $\sim$180 ps. The *trans-cis* photoisomerization through an inversion mechanism on the S_1 potential energy surface and the internal conversion from the S_1 state to the high vibrational state of the S_0 state are observed respectively. The time constant of $\sim$0.7 ps is the average timescale of these two decay pathways. And the $\sim$180 ps-component is assigned to an intersystem crossing from the S_1 state to the T_2 state. Finally, the timescale of the vibrational cooling process in the ground state of *cis* and *trans*-4-AAB are $\sim$4 and $\sim$13 ps respectively.

V. ACKNOWLEDGMENTS

[1] H. Rau, *Photochromism: Molecules and Systems*, Elsevier: Amsterdam, (1990).

[2] T. Ikeda and O. Tsutsumi, Science **268**, 1873 (1995).

[3] Z. Sekkat and M. Dumont, Appl. Phys. B **54**, 486 (1992).

[4] Z. F. Liu, K. Hashimoto, and A. Fujishima, Nature **347**, 658 (1990).

[5] L. Ulysse, J. Cubillos, and J. Chmielewski, J. Am. Chem. Soc. **117**, 8466 (1995).

[6] K. G. Sudesh and D. C. Neckers, Chem. Rev. **89**, 1915 (1989).

[7] H. Rau and E. Lüddecke, J. Am. Chem. Soc. **104**, 1616 (1982).

[8] H. Rau, J. Photochem. **26**, 221 (1984).

[9] N. Siampiringue, G. Guyot, S. Monti, and P. Bortolus, J. Photochem. **37**, 185 (1987).

[10] A. P. Prikhotko, V. A. Pavloshchuk, A. G. Tereshchenko, and L. I. Shanskii, Ukrain. Fiz. Z. **37**, 1822 (1992).

[11] I. K. Lednev, T. Q. Ye, L. C. Abbott, R. E. Hester, and J. N. Moore, J. Phys. Chem. A **102**, 9161 (1998).

[12] T. Nägele, R. Hoche, W. Zinth, and J. Wachtveitl, Chem. Phys. Lett. **272**, 489 (1997).

[13] I. K. Lednev, T. Q. Ye, P. Matousek, M. Towrie, P. Foggi, F. V. R. Neuwahl, S. Umapathy, R. E. Hester, and J. N. Moore, Chem. Phys. Lett. **290**, 68 (1998).

[14] I. K. Lednev, T. Q. Ye, R. E. Hester, and J. N. Moore, J. Phys. Chem. **100**, 13338 (1996).

[15] D. H. Waldeck, Chem. Rev. **91**, 415 (1991).

[16] T. Fujino, S. Y. Arzhantsev, and T. Tahara. J. Phys. Chem. A **105**, 8123 (2001).

[17] P. Hamm, S. M. Ohline, and W. Zinth, J. Chem. Phys. **106**, 519 (1997).

[18] H. Gorner, H. Gruen, and D. Schulte-Frohllnde, J. Phys. Chem. **84**, 3031 (1980).

[19] A. Angelo, F. Elisa, and P. Silvio, J. Chem. Soc. Perkin Trans. II 1021 (1983).

[20] J. Wachtveitl, T. Nägele, B. Puell, W. Zinth, M. Krüger, S. Rudolph-Böhner, D. Oesterhelt, and L. Moroder, J. Photochem. Photobiol. A **105**, 283 (1997).

[21] J. Azuma, N. Tamai, A. Shishido, and T. Ikeda, Chem. Phys. Lett. **288**, 77 (1998).

[22] S. G. Mayer, C. L. Thomsen, M. P. Philpott, and P. J. Reid, Chem. Phys. Lett. **314**, 246 (1999).

[23] N. Tamai and H. Miyasaka, Chem. Rev. **100**, 1875 (2000).

[24] H. Yasushi, Y. Hiroharu, and S. Tsuguo, J. Phys. Chem. A **106**, 3067 (2002).

[25] Z. R. Wei, F. Zhang, Y. M. Wang, and B. Zhang, Chin. J. Chem. Phys. **20**, 419 (2007).

[26] M. J. Frisch, G. W. Trucks, H. B. Schlegel, G. E. Scuseria, M. A. Robb, J. R. Cheeseman, G. Scalmani, V. Barone, B. Mennucci,G. A. Petersson, H. Nakatsuji, M. Caricato, X. Li, H. P. Hratchian, A. F. Izmaylov, J. Bloino, G. Zheng, J. L. Sonnenberg, M. Hada, M. Ehara, K. Toyota, R. Fukuda, J. Hasegawa, M. Ishida, T. Nakajima, Y. Honda, O. Kitao, H. Nakai, T. Vreven, J. A. Jr. Montgomery, J. E. Peralta, F. Ogliaro, M. Bearpark, J. J. Heyd, E. Brothers, K. N. Kudin, V. N. Staroverov, R. Kobayashi, J. Normand, K. Raghavachari, A. Rendell, J. C. Burant, S. S. Iyengar, J. Tomasi, M. Cossi, N. Rega, J. M. Millam, M. Klene, J. E. Knox, J. B. Cross, V. Bakken, C. Adamo, J. Jaramillo, R. Gomperts, R. E. Stratmann, O. Yazyev, A. J. Austin, R. Cammi, C. Pomelli, J. W. Ochterski, R. L. Martin, K. Morokuma, V. G. Zakrzewski, G. A. Voth, P. Salvador, J. J. Dannenberg, S. Dapprich, A. D. Daniels, O. Farkas, J. B. Foresman, J. V. Ortiz, J. Cioslowski, and D. J. Fox, *Gaussian 09, Revision A02*, Wallingford CT: Gaussian, Inc., (2009).